

Climate change projections for Greece in the 21st century from high-resolution EURO-CORDEX RCM simulations

Aristeidis K. Georgoulas^{a,*}, Dimitris Akritidis^a, Alkiviadis Kalisoras^a, John Kapsomenakis^b,
Dimitris Melas^c, Christos S. Zerefos^{b,d,e}, Prodromos Zanis^a

^a Department of Meteorology and Climatology, School of Geology, Aristotle University of Thessaloniki, Thessaloniki, Greece

^b Research Centre for Atmospheric Physics and Climatology, Academy of Athens, Athens, Greece

^c Laboratory of Atmospheric Physics, Physics Department, Aristotle University of Thessaloniki, Thessaloniki, Greece

^d Biomedical Research Foundation, Academy of Athens, Athens, Greece

^e Navarino Environmental Observatory, Costa Navarino, Messinia, Greece

ARTICLE INFO

Keywords:

Climate change
Greece
Temperature
Precipitation
Climate indices
EURO-CORDEX

ABSTRACT

We present an updated assessment of projected climate change over Greece in the near future and at the end of the 21st century, focusing on near surface temperature, precipitation, and related heat (Hot Days and Tropical Nights), cold (Frost Days), and drought (Consecutive Dry Days) climate indices. The analysis is based on an ensemble of 11 high-resolution EURO-CORDEX regional climate model (RCM) simulations covering the historical period 1950–2005 and the future period 2006–2100 under the influence of a strong, a moderate, and a no mitigation Representative Concentration Pathway (RCP2.6, RCP4.5 and RCP8.5). The statistical robustness of climate change signal is also assessed. Our results strongly point towards a warmer future for Greece under all the examined RCPs. Under RCP8.5, annual near surface temperature is projected to increase on average by 1.6 °C in the near future and 4.3 °C at the end of the century. As a consequence of warming, the number of hot days and tropical nights in a year is projected to increase significantly and the number of frost days to decrease. In addition, the future will be possibly drier. Statistically robust results for precipitation changes are found only for the end-of-the-century period under RCP8.5. Precipitation is generally projected to decrease under RCP8.5 by –16% and the number of consecutive dry days in a year to increase by 15.4 days (30%) at the end of the century.

1. Introduction

Today, it is widely discussed that we live in the so-called “Anthropocene”, an era where humans exert a significant impact on the Earth-Atmosphere system. During the Anthropocene, humans are contributing to climate change in various ways, the most notable being man-made global emissions of greenhouse gases (GHGs) (Hansen et al., 2007). The recently released Sixth Assessment Report (AR6) of the Intergovernmental Panel on Climate Change (IPCC, 2021) highlights more than ever the driving role of human activities in the observed climate change. AR6 suggests that the global near surface temperature has increased by ~1.1 °C relative to the late 19th century (1850–1900) almost exclusively due to human activities. At the same time hot extremes (including heat waves) have become more frequent and more intense across most land regions since the 1950s. Precipitation changes are more uncertain. According to AR6, global precipitation over land has

“likely” (probability >66%) increased since 1950 with humans contributing to the observed change. Regionally, precipitation change exhibits diverse patterns with areas that become drier or wetter.

The Mediterranean Basin, a widely recognized climate change hot spot (Giorgi, 2006), along with western North America, Central America, Europe, the Amazon, southern Africa, China, southeast Asia, and Australia, is one of the regions that becomes drier (Cook et al., 2020; Spinoni et al., 2020). A series of studies the last two decades, using global climate models (GCMs) and regional climate models (RCMs), point towards a warmer and drier future under various emission scenarios (Coppola et al., 2021; Cos et al., 2021; Diffenbaugh et al., 2007; Gao et al., 2006; Giannakopoulos et al., 2009; Gibelin and Déqué, 2003; Giorgi and Lionello, 2008; Goubanova and Li, 2007; Lelieveld et al., 2014; Lelieveld et al., 2012; Zittis et al., 2021; Zittis et al., 2019). The majority of the studies are based on RCMs as dynamical downscaling allows for a better representation of the local features, especially over

* Corresponding author.

E-mail address: ageor@auth.gr (A.K. Georgoulas).

<https://doi.org/10.1016/j.atmosres.2022.106049>

Received 15 November 2021; Received in revised form 14 January 2022; Accepted 20 January 2022

Available online 26 January 2022

0169-8095/© 2022 Elsevier B.V. All rights reserved.

areas with complex topography (Xue et al., 2014) like the greater area around Greece (hereafter denoted southeastern Europe) where we focus in this study. It is an area with steep orography from the mountainous regions to the coast, a long and convoluted coastline, and many small islands (Fig. 1). With a mean near surface temperature higher than ~ 1.5 °C relative to the preindustrial times, Mediterranean has already reached the tough target limit set out in the Paris Agreement in 2015 (MedECC, 2020) and the Mediterranean countries already experience the consequences of climate change. However, mitigation and adaptation strategies vary from country to country due to differences in the socioeconomic, cultural, and political status (MedECC, 2020 and references therein).

Greece, located in the heart of the Eastern Mediterranean, is experiencing the last decades an increasing number of various extreme events, directly or indirectly related to climate change (e.g., fires, floods, heat waves, etc.), and the public and political awareness about climate change is continuously increasing. The local scientific community has acknowledged the problem with several studies focusing on the country's past, current and future climate (Anagnostopoulou, 2017; Founda et al., 2019; Founda et al., 2004; Giannakopoulos et al., 2011; Nastos et al., 2011; Nastos and Kapsomenakis, 2015; Nastos and Zerefos, 2009; Politi et al., 2021; Tolika et al., 2012; Zanis et al., 2015; Zanis et al., 2009) the last two decades. In 2011, a detailed assessment of the past, present, and future of climate in Greece and the corresponding impacts on key sectors (e.g., fisheries and aquaculture, agriculture, tourism, transportation, and human health) was compiled from the Climate Change Impacts Study Committee on behalf of the Bank of Greece (CCISC, 2011). The cost of climate change for the period 2011–2100 was estimated at 578 to 701 billion euros (cost with and without any mitigation measures) which is about 3–4 times the country's gross domestic product (GDP) in 2020 (Eurostat, 2021).

Under these circumstances, 11 research entities united under the national project CLIMPACT (National Network on Climate Change and its Impacts; <https://climpact.gr>) in a coordinated effort to update our knowledge on climate change and its impacts in Greece and the surrounding areas. The research presented here was implemented within the framework of the project and constitutes the latest view into climate

change projections for Greece. It is expected to serve as a yardstick for upcoming CLIMPACT studies mostly focusing on the impacts of climate change on specific sectors of life, the economy, and the environment in Greece. The analysis is based on an ensemble of state-of-the-art high-resolution EURO-CORDEX RCM simulations. More specifically, the manuscript is organized as follows: first, we present the RCMs and the corresponding datasets used along with the methodology we followed. Then, the projected changes of near surface temperature, precipitation, and selected heat/cold and drought indices are presented for the near future and the end of the century. The main conclusions are summarized in the end.

2. Data and methods

2.1. Regional climate model simulations

For the scope of this research, daily mean, minimum and maximum near surface temperature (TAS, TASMIn and TASMAX; in °C) and precipitation (PR; in mm day⁻¹) data from 11 sets of RCM simulations implemented within the framework of the EURO-CORDEX initiative (<https://www.euro-cordex.net/>) are used. More specifically, the simulations used here cover the greater European area ($\sim 27^{\circ}\text{N}$ - 72°N , $\sim 22^{\circ}\text{W}$ - 45°E) at a fine horizontal resolution of 0.11° (~ 12.5 km) (Jacob et al., 2020; Jacob et al., 2014; Vautard et al., 2013). The simulations are a product of various RCMs driven by various GCMs (for details see Table 1). Each set incorporates four different simulations: a historical (Hist) simulation for the period 1950–2005 and three simulations for the period 2006–2100 under different RCPs (RCP2.6, RCP4.5 and RCP8.5) driven by a GCM. The GCM simulations, used to drive the RCMs, were implemented within the framework of the Coupled Model Intercomparison Project (CMIP5) project (Taylor et al., 2012) for the needs of the Fifth Assessment Report (AR5) of the Intergovernmental Panel on Climate Change (IPCC, 2013). Although regional analyses from the most recent CMIP6 AR6 GCM model projections are already published (Almazroui et al., 2021; Almazroui et al., 2020; Cos et al., 2021), their regionally downscaled projections within the CORDEX program are not yet available. RCPs are GHG concentration scenarios which refer to the radiative forcing caused by changes in atmospheric composition (Moss et al., 2010; van Vuuren et al., 2011a). Hence, RCP2.6 corresponds to radiative forcing of 2.6 W m^{-2} in the year 2100 relative to preindustrial times and so on. RCP2.6 is a strong mitigation scenario where GHG concentrations are bound to decrease by $\sim 70\%$ within the period 2010–2100 (van Vuuren et al., 2011b). On the contrary, RCP8.5 is a scenario without any future environmental and climate change policies where GHG concentrations increase (Riahi et al., 2011) while RCP4.5 is a moderate mitigation scenario, designed to be cost-efficient to reach the radiative forcing target of 4.5 W m^{-2} , where GHG concentrations start decreasing after 2040 (Thomson et al., 2011).

To gain confidence in the future projections presented here, the ability of the control (Hist) simulations to capture the basic characteristics of climate in Greece for the reference period 1971–2000 is examined (detailed results presented in the electronic supplement of the manuscript). TAS, TASMIn, TASMAX and PR from the Hist simulations are evaluated against gridded observational data at a 0.1° horizontal resolution from the latest release of the European Climate Assessment & Dataset (ECA&D) gridded dataset (E-OBS version 23.1e). In general, the E-OBS gridded dataset is constructed using observational data from stations all over Europe as described in Haylock et al. (2008) while details about the ensemble version used here are given in Cornes et al. (2018). Unlike single station measurements (Hadjinicolaou et al., 2017), the gridded observational data allow for a spatial evaluation of the high-resolution EURO-CORDEX RCM simulations used here. Overall, our ensemble temperature data exhibit a reasonable agreement with the E-OBS data while the PR data show a moderate agreement following previous EURO-CORDEX studies (Katragkou et al., 2015; Kotlarski et al., 2014).

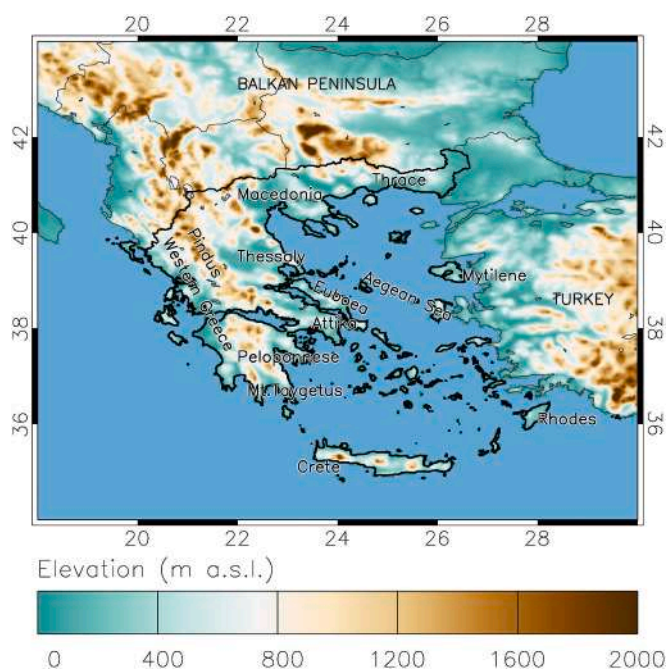


Fig. 1. Topography of the region under study (in meters above sea level - m a.s.l.). Locations and areas of interest mentioned in the text are also indicated along with the outline of Greece.

Table 1

List with the 11 EURO-CORDEX sets of simulations used in the present study.

	RCM	Driving GCM	Realization	Hist	RCP2.6	RCP4.5	RCP8.5
1	ALADIN63.v2	CNRM.CNRM-CERFACS-CNRM-CM5	r1i1p1	x	x	x	x
2	CCLM4-8-17.v1	CLMcom.ICHEC-EC-EARTH	r12i1p1	x	x	x	x
3	HIRHAM5.v2	DMLI.ICHEC-EC-EARTH	r3i1p1	x	x	x	x
4	RACMO22E.v1	KNMI.ICHEC-EC-EARTH	r12i1p1	x	x	x	x
5	RACMO22E.v2	KNMI.MOHC-HadGEM2-ES	r1i1p1	x	x	x	x
6	RACMO22E.v2	KNMI.CNRM-CERFACS-CNRM-CM5	r1i1p1	x	x	x	x
7	RCA4.v1	SMHI.MOHC-HadGEM2-ES	r1i1p1	x	x	x	x
8	RCA4.v1	SMHI.MPI-M-MPI-ESM-LR	r1i1p1	x	x	x	x
9	RCA4.v1	SMHI.ICHEC-EC-EARTH	r12i1p1	x	x	x	x
10	REMO2009.v1	MPI-CSC.MPI-M-MPI-ESM-LR	r1i1p1	x	x	x	x
11	REMO2009.v1	MPI-CSC.MPI-M-MPI-ESM-LR	r2i1p1	x	x	x	x

2.2. Methodology

In this work, changes in climate related parameters over Greece are reported for the near-future (2021–2050) and the end-of-the-century (2071–2100) 30-year periods relative to the reference period (1971–2000). The original EURO-CORDEX daily data were brought to a standard $0.1^\circ \times 0.1^\circ$ grid using bilinear interpolation focusing on southeastern Europe (34°N - 44°N , 18°E - 30°E) with Greece being in the center of this region (Fig. 1; locations and areas of interest mentioned in the text are also indicated in the figure). Data from the 11 sets of simulations were merged in order to compile an ensemble dataset for the historical period (1950–2005) and for each RCP separately that spans from 2006 to 2100.

The projected changes for TAS and PR for the near future and the end of the century are expressed by the difference between the two periods and the reference period for the ensemble data. The changes are calculated on an annual and seasonal basis for each grid cell and each RCP separately, and the results are presented by means of maps (in the main text and in the electronic supplement of the manuscript). The statistical robustness of the differences is also checked taking into account the ensemble's inter-model variability similarly to previous studies (Jacob et al., 2014; Pfeifer et al., 2015; Spinoni et al., 2020). Specifically, a difference is considered robust if the differences for at least 7 out of the 11 simulations constituting each ensemble have the same sign with the ensemble difference and are statistically significant at the 95% confidence level according to the non-parametric Mann-Whitney test (Mann and Whitney, 1947). In addition, in order to generalize our results, ensemble timeseries with the difference between the annual means and the mean for the reference period 1971–2000 for Greece (land only areas) are also presented for the 150-year period 1950–2100 including all RCPs. The timeseries are presented on an annual basis and for each season, separately. The ensemble mean difference of the periods 2021–2050 and 2071–2100 with the reference period for Greece along with the corresponding median difference, the 25th and 75th percentiles and the maximum and minimum difference values from the 11 simulations constituting each ensemble (inter-model variability) are presented by means of boxplots and are given in Table 2.

The same analysis was repeated for a number of climatic indices which were calculated on an annual basis from TASMIn, TASMx and PR and express heat, cold and drought extremes. The definition of these indices comes from the European Climate Assessment (ECA) project. More specifically, Hot Days (HD) expresses the number of days within a year where TASMx is greater than 35°C , Tropical nights (TR) expresses the number of days within a year where TASMIn is greater than 20°C , Frost Days (FD) expresses the number of days within a year where TASMIn is below 0°C and Consecutive Dry Days (CDD) expresses the number of consecutive days within a year where PR is lower than 1 mm. The indices were calculated for each one of the RCM simulations separately and then they were averaged to compile the ensemble mean values.

3. Results and discussion

3.1. Projected temperature change

In Fig. 2, the projected ensemble TAS change for the near-future and the end-of-the-century periods are shown for the three RCPs on an annual basis. A statistically robust TAS increase is indicated over the whole domain for both the examined periods (near future and the end of the century) and under all the examined RCPs. An increase of $1\text{--}1.5^\circ\text{C}$ is projected over the whole southeastern Europe domain in the near future (2021–2050) relative to the reference period (1971–2000) based on RCP2.6. Similarly, an increase of $1\text{--}1.5^\circ\text{C}$ over the whole domain is also indicated in the RCP4.5 projections reaching values up to $1.5\text{--}2.0^\circ\text{C}$ over the Pindus Mountain Range in Greece and other high altitude areas in the Balkan Peninsula and Turkey. In the case of RCP8.5, a TAS increase of $1.5\text{--}2.0^\circ\text{C}$ is indicated over all the continental areas and over the Black Sea and $1.0\text{--}1.5^\circ\text{C}$ over the rest of the sea areas. At the end of the century (2071–2100), a TAS increase of $1\text{--}1.5^\circ\text{C}$ is projected over the whole southeastern Europe domain according to RCP2.6. For RCP4.5, the projected increase is $2.0\text{--}2.5^\circ\text{C}$, especially over continental areas, while, over some high altitude areas it may be up to $2.5\text{--}3.0^\circ\text{C}$. For RCP8.5, the projected TAS increase is larger, ranging from 3.0 to 3.5°C , mostly over the sea, up to $4.5\text{--}5.0^\circ\text{C}$ over mountainous areas. Generally, TAS is projected to increase by $4.0\text{--}4.5^\circ\text{C}$ over the continental areas.

Specifically for Greece (land areas only), Fig. 2g presents the timeseries of the difference between annual TAS from the reference period (1971–200) mean TAS for the period 1950–2100. As shown in the boxplot (dots) embedded in Fig. 2g, for RCP2.6, an average increase of 1.2°C and 1.4°C is projected for the near future and the end of the century, respectively. For RCP4.5, the projected TAS increase is 1.4°C and 2.3°C , respectively, while, for RCP8.5, 1.6°C and 4.3°C , respectively. These values along with the corresponding median difference, the 25th and 75th percentiles and the maximum and minimum difference values from the 11 simulations constituting each ensemble (inter-model variability) also appear in Table 2. It is quite obvious that according to the strong and moderate mitigation scenarios (RCP2.6 and RCP4.5, respectively), TAS either nearly stabilizes since the middle of the 21st century or increases at a slower pace following the gradual decrease of GHG emissions compared to the no-mitigation RCP8.5 scenario where TAS increases steadily following the increase of GHG emissions. It merits to be mentioned here that the skewness of the distribution of the TAS differences between the future and reference periods appearing in Fig. 2g is positive (mean value higher than the median). This indicates that a minority from the RCM simulations that constitute the ensemble drags the mean to a higher value while the majority of the simulations have lower values. Similar conclusions can be reached for the other basic parameter, PR, which is examined in the next section.

While TASMIn and TASMx data are primarily used for the calculation of the climatic indices in this paper, it merits to be mentioned that the same analysis with TAS was also applied on these two parameters.

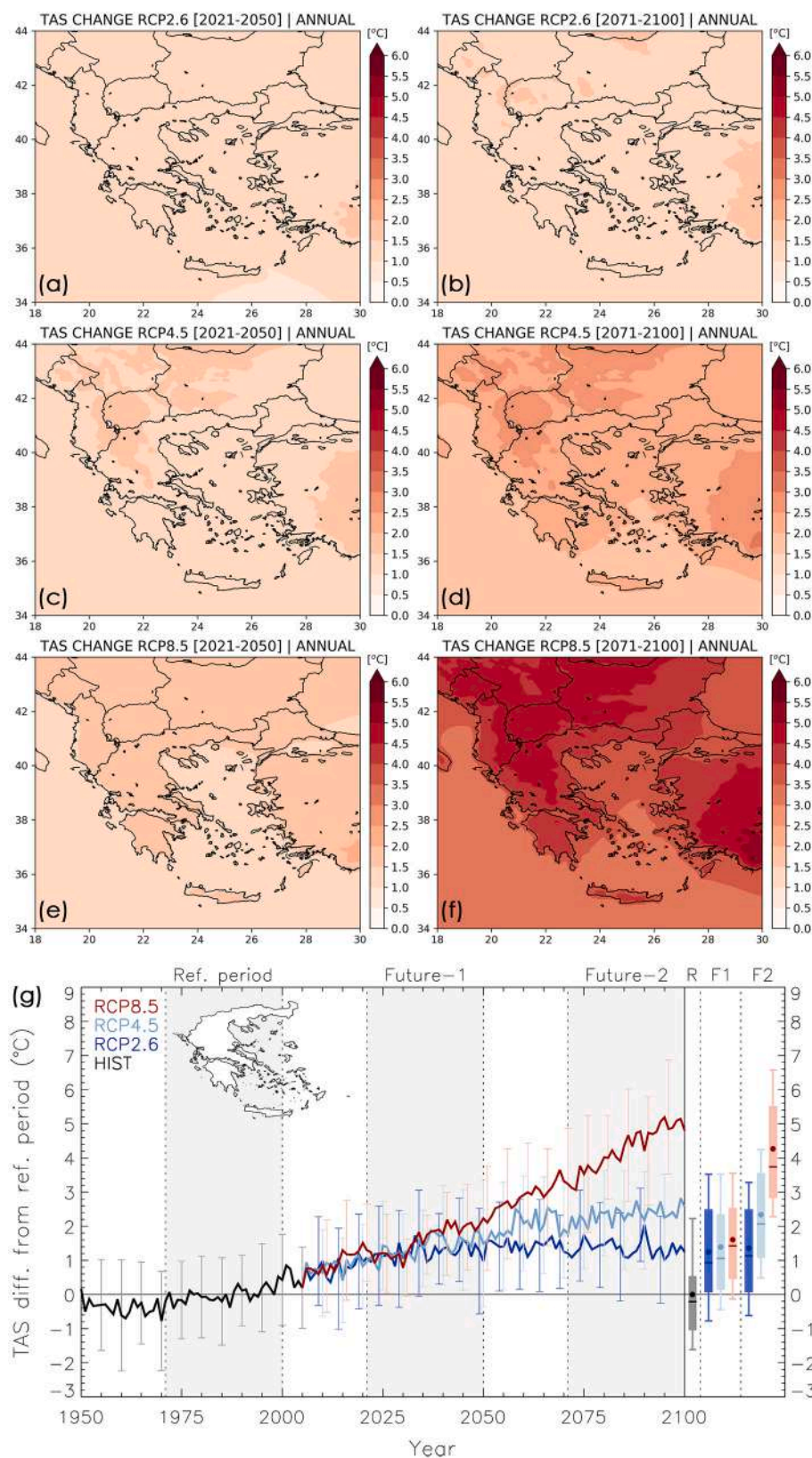


Fig. 2. Difference in the TAS fields from the EURO-CORDEX ensemble between the near-future (2021–2050) and the reference period (1971–2000) for southeastern Europe for RCP2.6 (a). (b) the same as (a) but for the difference between the end-of-the-century (2071–2100) and the reference period. (c) and (d) the same as (a) and (b) respectively but for RCP4.5. (e) and (f) the same as (a) and (b) respectively but for RCP8.5. Hatching indicates areas where the differences are not statistically robust. (g) time-series (1950–2100) with the difference between the annual mean TAS and the mean TAS for the reference period (1971–2000) for Greece (land only; boundaries shown in the figure). Error bars denote the $\pm 1\sigma$ from the 11 EURO-CORDEX simulations annual means and are plotted every 5 years. The boxplot on the right shows the mean difference (dot) of the periods 1971–2000, 2021–2050 and 2071–2100 with the reference period. The middle lines in each box represent the corresponding median difference, the boxes indicate the range between the 25th and 75th percentiles and the whiskers the maximum and minimum difference values from the 11 EURO-CORDEX simulations (inter-model variability).

The projected TASMIN and TASMAX changes (Figs. S3-S6) are pretty similar to the TAS ones. In addition, the seasonal analysis revealed that the TAS change patterns are pretty similar throughout all the seasons

(Figs. S7-S10) with the annual change patterns (Fig. 2) but in summer (June-July-August) the projected changes are larger, particularly under RCP4.5 and RCP8.5. Under RCP2.6, the average projected TAS change

Table 2

Mean value for Greece (land areas only) of TAS (in °C), PR (in mm day⁻¹), and the different climatic indices (HD, TR, FD and CDD in days) examined here from the EURO-CORDEX ensemble for the reference period (1971–2000; Historical simulations) and for the near-future (2021–2050) and the end-of-the-century (2071–2100) period under different RCPs. The ensemble mean difference ($\pm 1\sigma$) and percentage difference (in %) of the near-future and the end-of-the-century with the reference period is also given along with the corresponding minimum and maximum difference, the median difference, and the 25th and 75th percentiles values from the 11 simulations constituting each ensemble (inter-model variability).

Param.	Mode	Period	Mean	Mean diff. $\pm 1\sigma$	% diff.	Min diff.	Max diff.	Median diff.	Pctl25 diff.	Pctl75 diff.
TAS	Hist	1971–2000	13.0	0.0 \pm 1.7	0	-1.6	2.2	-0.2	-1.0	0.5
TAS	RCP26	2021–2050	14.3	1.2 \pm 1.8	10	-0.8	3.5	0.9	-0.1	2.2
TAS	RCP26	2071–2100	14.4	1.4 \pm 1.7	10	-0.6	3.3	1.1	0.1	2.5
TAS	RCP45	2021–2050	14.4	1.4 \pm 1.8	11	-0.4	3.5	1.1	0.1	2.3
TAS	RCP45	2071–2100	15.4	2.3 \pm 1.7	18	0.5	4.2	2.1	1.1	3.6
TAS	RCP85	2021–2050	14.6	1.6 \pm 1.7	12	-0.1	3.6	1.4	0.5	2.5
TAS	RCP85	2071–2100	17.3	4.3 \pm 1.9	33	2.3	6.6	3.7	2.8	5.5
PR	Hist	1971–2000	2.4	0.0 \pm 0.6	0	-0.6	1.2	0.0	-0.4	0.1
PR	RCP26	2021–2050	2.3	-0.1 \pm 0.7	-3	-0.6	1.1	-0.2	-0.5	0.2
PR	RCP26	2071–2100	2.4	0.0 \pm 0.6	0	-0.6	1.2	-0.1	-0.4	0.2
PR	RCP45	2021–2050	2.3	-0.1 \pm 0.6	-3	-0.6	1.2	-0.1	-0.5	0.2
PR	RCP45	2071–2100	2.2	-0.1 \pm 0.7	-6	-0.7	1.2	-0.2	-0.5	0.0
PR	RCP85	2021–2050	2.3	-0.1 \pm 0.6	-3	-0.6	1.1	-0.2	-0.4	0.2
PR	RCP85	2071–2100	2.0	-0.4 \pm 0.7	-16	-0.9	0.9	-0.5	-0.8	-0.1
HD	Hist	1971–2000	5.1	0.0 \pm 6.9	0	-4.8	9.8	-1.7	-3.9	0.6
HD	RCP26	2021–2050	10.6	5.5 \pm 9.9	108	-4.3	22.5	3.6	-2.7	10.4
HD	RCP26	2071–2100	10.2	5.1 \pm 9.5	99	-4.5	20.9	3.5	-2.5	9.7
HD	RCP45	2021–2050	11.9	6.7 \pm 10.2	132	-4.0	23.5	5.5	-2.1	11.4
HD	RCP45	2071–2100	16.9	11.8 \pm 13.5	232	-3.1	34.5	10.8	-0.8	23.0
HD	RCP85	2021–2050	12.6	7.4 \pm 10.9	146	-4.1	26.9	6.5	-2.7	13.8
HD	RCP85	2071–2100	34.5	29.4 \pm 20.3	577	3.7	61.2	25.2	7.9	48.3
TR	Hist	1971–2000	21.3	0.0 \pm 12.6	0	-13.3	14.5	-1.6	-6.3	7.0
TR	RCP26	2021–2050	36.0	14.7 \pm 16.5	69	-7.4	33.8	15.0	2.6	28.4
TR	RCP26	2071–2100	35.9	14.6 \pm 16.3	69	-8.7	31.7	16.9	4.5	29.2
TR	RCP45	2021–2050	38.2	16.9 \pm 16.1	79	-5.2	35.2	16.0	4.5	29.1
TR	RCP45	2071–2100	49.8	28.5 \pm 18.8	134	0.7	47.9	28.4	13.5	46.3
TR	RCP85	2021–2050	40.9	19.7 \pm 16.8	92	-3.8	39.2	18.6	6.1	32.7
TR	RCP85	2071–2100	79.1	57.9 \pm 21.0	272	26.8	80.9	61.0	34.6	76.9
FD	Hist	1971–2000	45.0	0.0 \pm 26.0	0	-30.2	27.0	-3.4	-9.9	18.0
FD	RCP26	2021–2050	35.4	-9.7 \pm 24.3	-21	-33.7	18.2	-11.4	-18.5	1.5
FD	RCP26	2071–2100	32.6	-12.4 \pm 23.3	-28	-33.8	12.3	-15.5	-21.2	-3.9
FD	RCP45	2021–2050	33.5	-11.6 \pm 24.0	-26	-35.1	12.1	-14.9	-19.7	-1.8
FD	RCP45	2071–2100	26.4	-18.6 \pm 21.6	-41	-35.7	1.7	-21.0	-25.3	-10.5
FD	RCP85	2021–2050	32.2	-12.9 \pm 23.1	-29	-33.7	9.3	-12.5	-25.2	-4.6
FD	RCP85	2071–2100	16.2	-28.8 \pm 20.7	-64	-42.0	-12.8	-29.1	-35.6	-23.7
CDD	Hist	1971–2000	51.0	0.0 \pm 14.9	0	-20.1	14.8	-2.0	-4.1	12.6
CDD	RCP26	2021–2050	52.6	1.6 \pm 14.7	3	-19.0	19.3	0.6	-6.3	11.1
CDD	RCP26	2071–2100	51.9	0.9 \pm 14.0	2	-18.8	13.5	-0.8	-4.8	9.5
CDD	RCP45	2021–2050	55.0	4.0 \pm 14.4	8	-17.6	19.8	4.0	0.5	12.6
CDD	RCP45	2071–2100	56.5	5.6 \pm 15.0	11	-18.8	19.9	6.7	-3.2	14.9
CDD	RCP85	2021–2050	55.2	4.2 \pm 14.7	8	-18.0	18.1	6.6	-3.1	12.2
CDD	RCP85	2071–2100	66.3	15.4 \pm 18.5	30	-14.2	34.1	18.1	0.4	29.4

for Greece is ~ 1.0 – 1.5 °C for all the seasons for the near-future and the end-of-the-century periods, being higher in summer (1.5 °C). For RCP4.5, the projected TAS change is 1.7 °C in the near future and 2.7 °C at the end of the century for summer. The corresponding changes are 1.9 °C and 5.2 °C for RCP8.5 (Fig. S11). Hence, the projected TAS change in summer is about 20% larger than the annual projected change for RCP4.5 and RCP8.5.

Our results are in accordance to the findings of Zittis et al. (2019). They used a multi-model and multi-domain ensemble to study the TAS and PR future changes over the whole Mediterranean Basin under the same RCPs with us. Other works, more focused on Greece, generally use lower spatial resolution RCM simulations under the older generation of IPCC's GHG emission scenarios (Special Report on Emissions Scenarios; SRES) (Tolika et al., 2012; Zanis et al., 2009; Zerefos et al., 2011). All these studies suggest a warmer future, the magnitude of the projected warming (values around 4 °C for the end of the century) largely depending on the specific RCM simulations that were used and the different SRES scenarios. More recently, Zanis et al. (2015) implemented simulations at a higher resolution (10 km) with an RCM for Greece under the A1B scenario (lies between RCP6.0 and RCP8.5) suggesting a TAS increase over continental areas of less than 1.8 °C for the period 2021–2050 and up to 4.2 °C for the period 1971–2100 relative to

1961–1990. In agreement to our results, these studies point towards a larger TAS increase for summer relative to the other seasons.

3.2. Projected precipitation change

Fig. 3 shows the projected ensemble PR change for the near-future and the end-of-the-century periods for the three RCPs on an annual basis. Following other climate change studies, the annual PR changes are primarily expressed as percentage differences (in %). The actual differences (in mm day⁻¹) are given for both the annual and seasonal PR changes in the main text and the electronic supplement (Figs. S12–S17). Unlike TAS, our analysis does not reveal a homogeneously distributed change signal over the whole southeastern Europe but areas with increasing and decreasing PR levels. The projected changes under the examined scenarios are generally statistically non-robust except for very limited areas over the sea and for RCP8.5 at the end of the century (2071–2100), where large areas in Greece and Turkey are projected to experience dryness (Figs. 3f and S12f). Concerning RCP2.6, for the near-future period (2021–2050) a non-robust PR decrease of 0 to -9% (0 to -1 mm day⁻¹) is projected over a large part of southeastern Europe, including Greece, and over the sea for latitudes below $\sim 39^\circ\text{N}$. On the contrary, a non-robust increase is projected over the northern Balkan

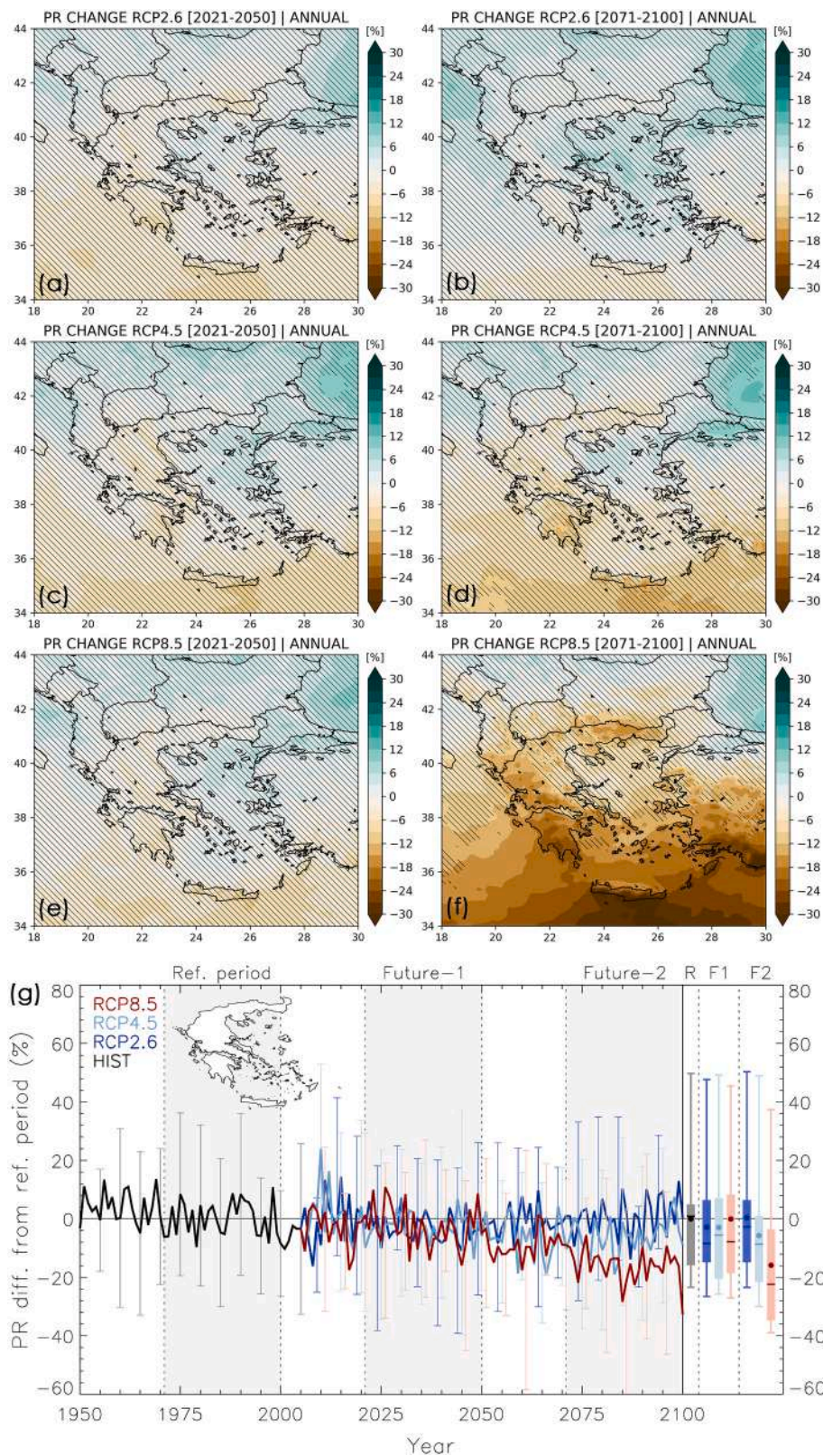


Fig. 3. The same as Fig. 2 but for PR.

Peninsula, the northern Aegean Sea, and areas over and around the Black Sea. For the end of the century, a non-robust increase of 0–12% (0–3 mm day⁻¹) is projected over southeastern Europe except for some areas in Greece (e.g. Eastern Macedonia and Thrace, Peloponnese, Attica), Turkey and over the sea for latitudes below ~36°N where a non-

robust decrease of 0 to –6% (0 to –1 mm day⁻¹) is projected. For RCP4.5, the PR change patterns for the near future are similar to the RCP2.6 ones for the same period. For the end-of-the-century period we observe a decrease of PR over Greece (especially over western Greece, Pindus Mountain Range, Peloponnese, and Crete), over areas in Turkey

and over the sea below 38–40°N. Over Greece, a statistically robust PR decrease of -15% (-0.7 mm day^{-1}) is indicated over Mount Taygetus in southern Peloponnese and over mountainous areas in Crete (up to -18%). RCP8.5 exhibits similar change patterns with the other two scenarios for the near-future period, but, for the end of the century a statistically robust decrease of PR is projected over Greece, southern Turkey and over the sea below $\sim 38^\circ\text{N}$. In Greece, the PR decrease reaches values from -20% up to -30% (-1 mm day^{-1}) over areas like Pindus, western Greece, Peloponnese, and Crete and areas in northern Greece. Over the sea, the robust decrease reaches values up to -30% (from -0.1 up to -0.4 mm day^{-1}). Overall, the future PR percentage decrease exhibits a north-to-south gradient as precipitation levels are generally lower in the South (Fig. 3f). The actual PR decrease (in mm day^{-1}) is more prominent over high elevation mountainous areas where precipitation levels are higher as shown in Fig. S12f.

Specifically, for Greece (land only areas), it can be seen in Fig. 3g that under RCP2.6 PR is projected to decrease by -3% (-0.1 mm day^{-1}) in the near-future period and then increase reaching the same levels with the reference period. For RCP4.5, a decrease of -3% and -6% is projected in the near future and at the end of the century, respectively. For RCP8.5, a PR decrease of -3% (-0.1 mm day^{-1}) is indicated again in the near future, but, at the end of the century a stronger decrease of -16% (-0.4 mm day^{-1}) is projected (Figs. 3g and S12g, and Table 2).

The seasonal analysis (Figs. S13–S16) showed that the PR change patterns are mostly driven by the winter (December–January–February) patterns and secondarily by the spring (March–April–May) and autumn (September–October–November) patterns. In winter, when PR levels peak, a statistically robust PR decrease well above -1 mm day^{-1} appears over southern Peloponnese, Crete, and southern Turkey for the end-of-the-century period under RCP8.5. In summer, a robust PR decrease ranging from 0 to -1.0 mm day^{-1} (patchy patterns) is indicated over all the continental areas under RCP8.5. The average projected PR change for Greece (land areas) for all the scenarios is pretty small throughout all the seasons except for RCP8.5 for the end-of-the-century period (Fig. S17). A clear decrease of -14% (-0.5 mm day^{-1}) is indicated for winter, -17% (-0.4 mm day^{-1}) for spring, -38% (-0.3 mm day^{-1}) for summer and -11% (-0.3 mm day^{-1}) for autumn. It is quite obvious that the projected percentage decrease of PR under RCP8.5 at the end of the century is larger in summer which is already a dry season for the area.

The decrease of PR in the future over Greece, as part of the Mediterranean Basin, was also seen in previous RCM ensemble studies under the RCP2.6, RCP4.5, and RCP8.5 scenarios (Jacob et al., 2014; Zittis et al., 2021; Zittis et al., 2019). The same stands for the general lack of statistical robustness except for RCP8.5. More local studies, focusing on Greece, have also reported a future PR decrease under the “old” IPCC SRES scenarios. Zanis et al. (2009) using an ensemble of RCM simulations under the A2 SRES scenario reported that PR will decrease by the end of the century relative to 1961–1990 by -15.8% . Under the A1B scenario, Tolika et al. (2012) suggested a PR decrease of -15.1% in winter and -36.9% in summer by the end of the century while Zanis et al. (2015) a decrease of -10 to -40% on an annual basis over different areas within southeastern Europe.

It has to be noted that apart from PR, the projected changes in the frequency of occurrence of very heavy precipitation days (days where PR exceeds 20 mm) on an annual basis were also examined within CLIMPACT. In general, the patterns (Fig. S18) are pretty similar to that of the actual PR change (Fig. S12f). Over Greece, a statistically robust change (decrease up to -4 days) appears only over high elevation mountainous areas in western Greece, Peloponnese, and Crete for the end-of-the-century period under RCP8.5. For the country as a whole (land areas), an average decrease of -1.3 days (-13%) is projected for the number of very heavy precipitation days in a year at the end of the century under RCP8.5 (see Fig. S19). Despite the projected decrease of PR and the frequency of very heavy precipitation events, Zittis et al. (2021) suggest that the intensity of individual events will increase during the second half or the 21st century under RCP8.5.

3.3. Projected changes in Hot Days and Tropical Nights

To assess the heat-extreme changes projected under the three RCPs examined here for the near-future and end-of-the-century periods the HD and TR climatic indices are examined on an annual basis. It is seen in Fig. 4 that under all RCPs and for both the examined future periods the HD change is largely statistically robust over the continental areas and non-robust almost everywhere over the sea. Following TASMEX, HD is projected to increase all over the southeastern Europe in line with previous studies (Lelieveld et al., 2014; Lelieveld et al., 2012). An increase of HD from 6 to 18 days appears over low elevation continental areas under RCP2.6 for both the future periods. Similar change patterns are projected for the near future under RCP4.5 while for the end of the century larger HD changes are projected over the low elevation areas ranging from 6 up to 36 days. For RCP8.5 the change patterns are similar to the RCP2.6 and RCP4.5 ones for the near-future period while for the end-of-the-century period large changes ranging from 6 up to 60 days are projected. Over Greece, the two most important HD change hotspots are the plains of the Thessaly and Central Macedonia (HD increase from 48 up to 60 days), with other areas in northern and western Greece and the Peloponnese following. Our results are close to that of Zerefos et al. (2011). In the timeseries shown in Fig. 4g for Greece, in line with TASMEX, under RCP2.6 and RCP4.5, HD either stabilizes since the middle of the 21st century or increases at a slower pace following the gradual decrease of GHG emissions while under RCP8.5 HD increases steadily following the steady increase of GHG emissions. Under RCP2.6, HD over Greece is projected to increase on average by 5.5 days (108%) in the near future and by 5.1 days (100%) at the end of the century. For RCP4.5, the corresponding increase is 6.7 days (131%) for the near-future and 11.8 days (231%; more than double relative to the reference period) for the end-of-the-century period. Under RCP8.5, HD is projected to increase by 7.4 days (145%) in the near future and by 29.4 days (576%; almost six times that of the reference period) at the end of the century (Fig. 4g and Table 2). Previous studies also pointed towards an increase of HD in the future. For example, Giannakopoulos et al. (2011) using simulations from a single RCM under the IPCC’s SRES A1B scenario found an increase of HD for the near future period 2021–2050 relative to 1961–1990 of 10 to 20 days over different locations in Greece. More recently, Zanis et al. (2015) reported an HD increase of 14 to 28 days for the period 2021–2050 and 49 to 63 days for the period 1971–2100 relative to 1961–1990.

For the second heat-related index examined here, TR, the change patterns are similar for all the scenarios and future periods with HD over land. Over the sea, a statistically robust TR increase ranging from 20–25 days (under RCP2.6 for both the future periods, and RCP4.5 for the near-future period) to values higher than 60 days (RCP8.5 for the end of the century) is indicated (Fig. 5). Over the continental heat extreme hot spots, the largest TR increase appears at the end of the century under RCP4.5 (up to 45 days) and particularly RCP8.5 (up to 80 days). Even under the strong mitigation scenario (RCP2.6), TR is projected to increase by up to 25 days for both the future periods over some areas. Under RCP2.6, TR over Greece is projected to increase on average by 14.7 days (69%) in the near future and remain at the same levels until the end of the century. For RCP4.5, the corresponding increase is 16.9 days (79%) for the near-future and 28.5 days (134%) for the end-of-the-century period. Under RCP8.5, a TR increase of 19.7 days (92%) in the near future and 57.9 days (272%; almost three times that of the reference period) at the end of the century (Fig. 5g and Table 2) is projected in line with the findings of Founda et al. (2019). Previous studies, based on RCM simulations under the SRES A1B scenario, also reported an increase of TR over Greece up to one month in the middle of the century and up to two months at the end of the century (Giannakopoulos et al., 2011; Lelieveld et al., 2012; Nastos and Kapsomenakis, 2015; Zanis et al., 2015; Zerefos et al., 2011).

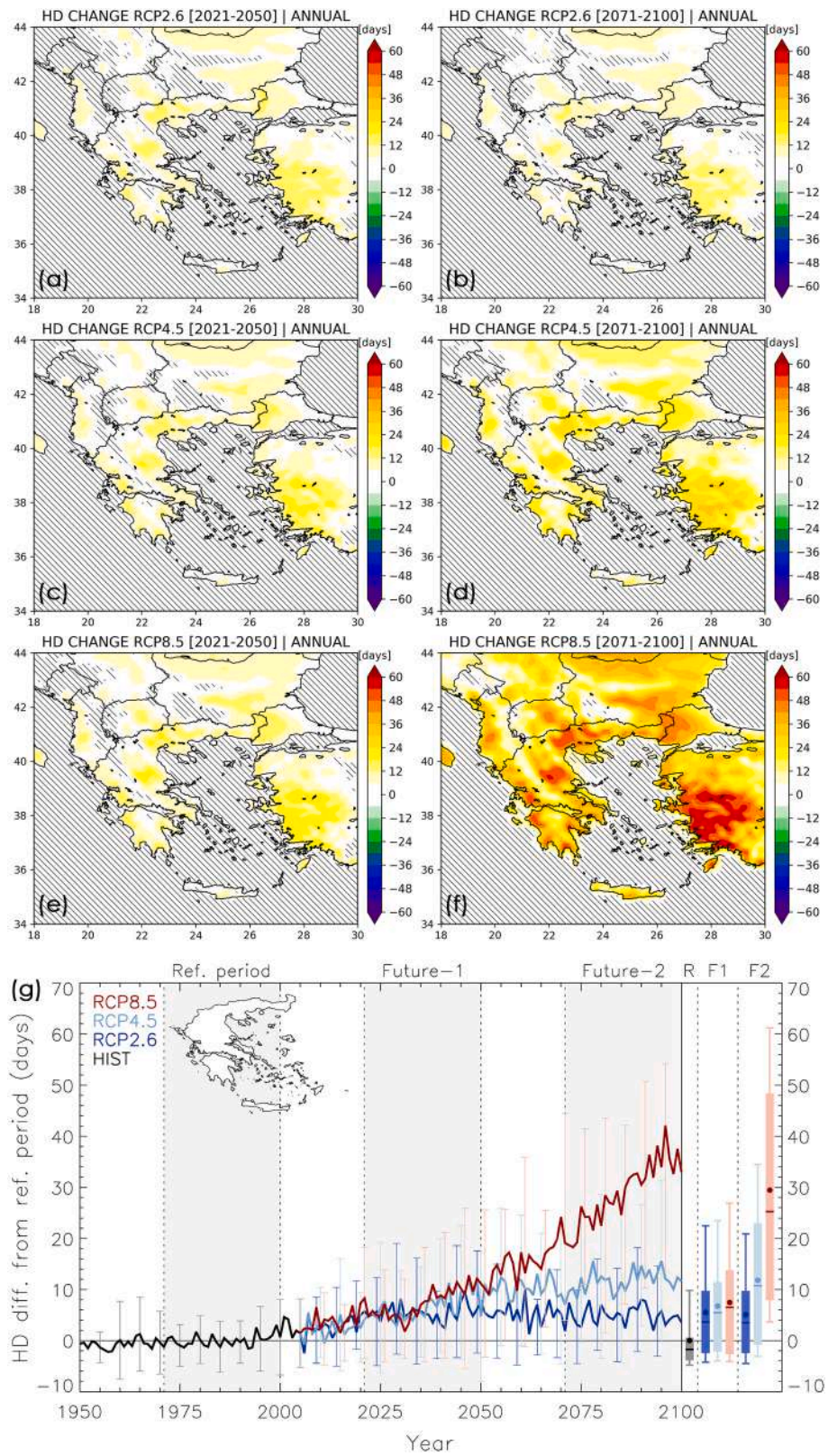


Fig. 4. The same as Fig. 2 but for HD.

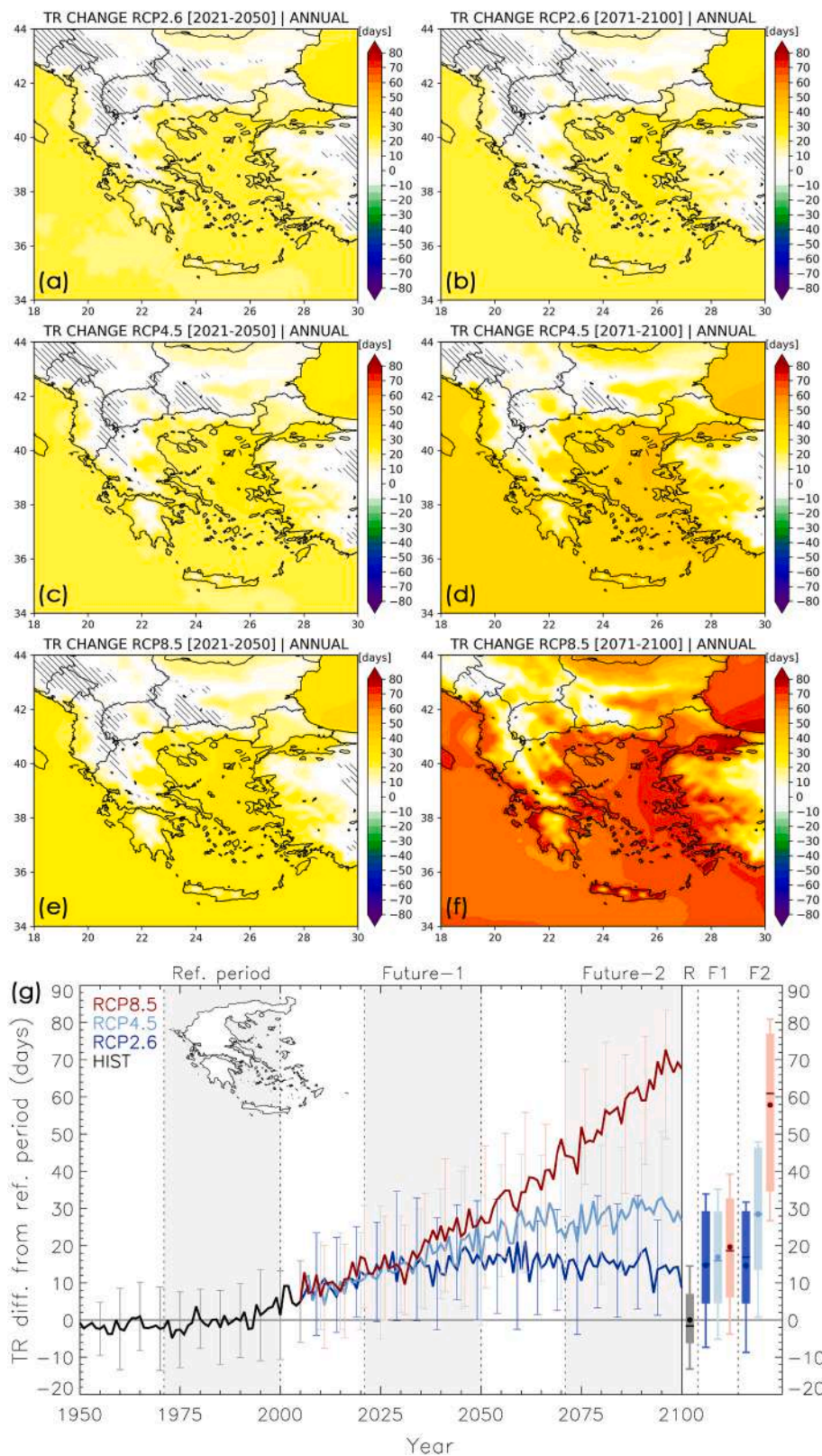


Fig. 5. The same as Fig. 2 but for TR.

3.4. Projected changes in Frost Days

Changes in cold extremes projected over southeastern Europe for the near-future and end-of-the-century periods under the three RCPs are assessed here by examining the FD climatic index. For all the cases,

changes in FD are largely statistically non-robust over the sea while over land a statistically robust decrease is indicated (Fig. 6). The FD change patterns resemble those of HD and TR with a decrease of -10 up to -30 days appearing over high elevation areas over land under RCP2.6 for both the future periods and under RCP4.5 for the near-future period. For

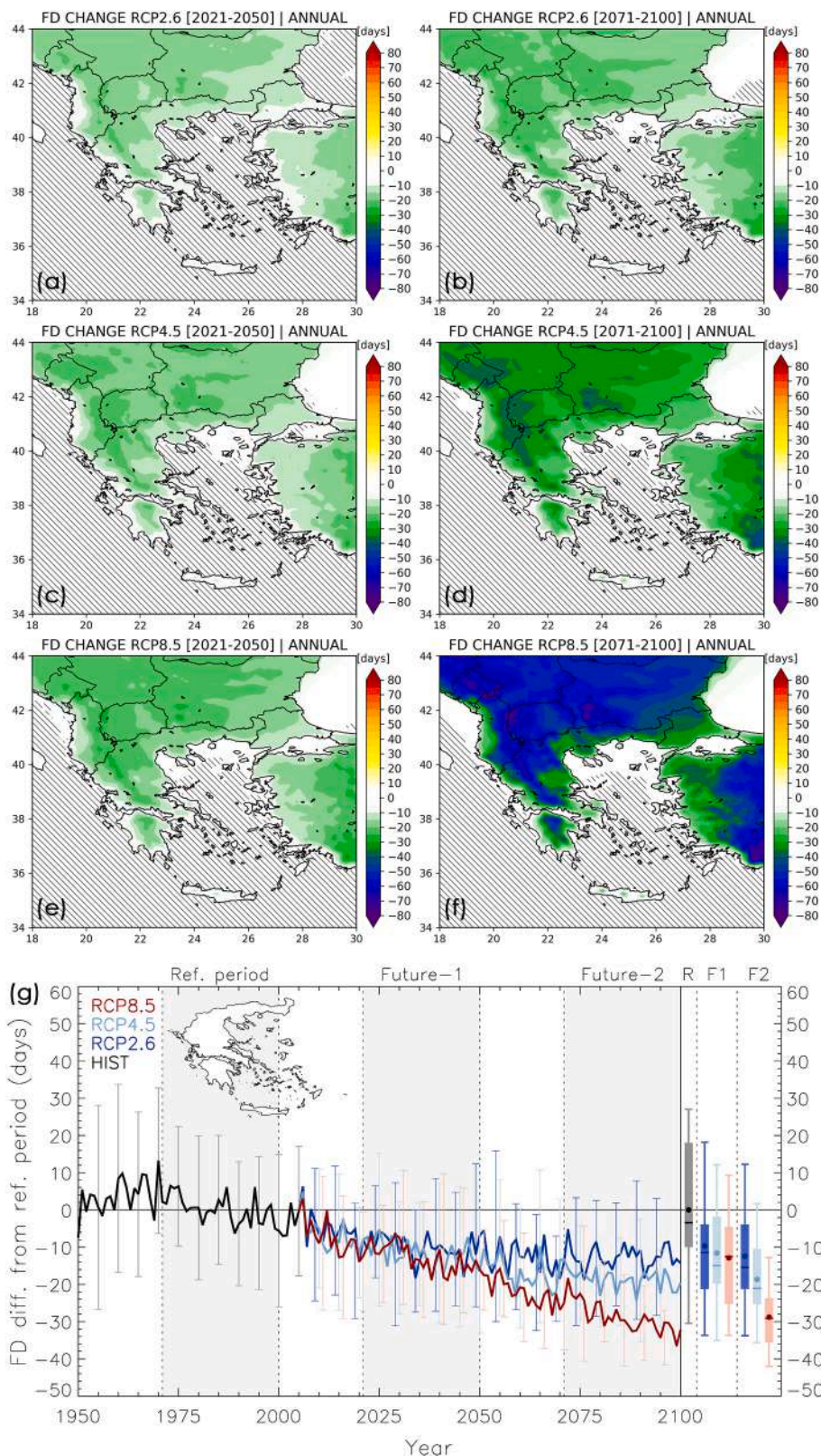


Fig. 6. The same as Fig. 2 but for FD.

RCP4.5, a larger decrease of -25 up to -60 days is projected over mountainous areas for the end-of-the-century period. For RCP8.5, the change patterns (not values) are similar to the RCP4.5 ones for the near-future period while for the end of the century a large decrease ranging from -50 up to -80 days is projected. Specifically, for Greece, under

RCP2.6, FD is projected to decrease on average by -9.7 days (-21%) in the near future and -12.4 days (-28%) at the end of the century. For RCP4.5, the corresponding decrease is -11.6 days (-26%) for the near-future and -18.6 days (-41%) for the end-of-the-century period. Under RCP8.5, FD decreases by -12.9 days (-29%) in the near future and by

−28.8 days (−64%) at the end of the century (Fig. 6g and Table 2). The values given here are in accordance to results from previous RCM studies under the SRES A1B scenario that focus on Greece (Giannakopoulos et al., 2011; Zanis et al., 2015; Zerefos et al., 2011).

3.5. Projected changes in Consecutive Dry Days

Following PR, changes in the CDD index, which is examined here to assess changes in drought extremes, are statistically significant over continental and sea areas under RCP8.5 and for the end of the century

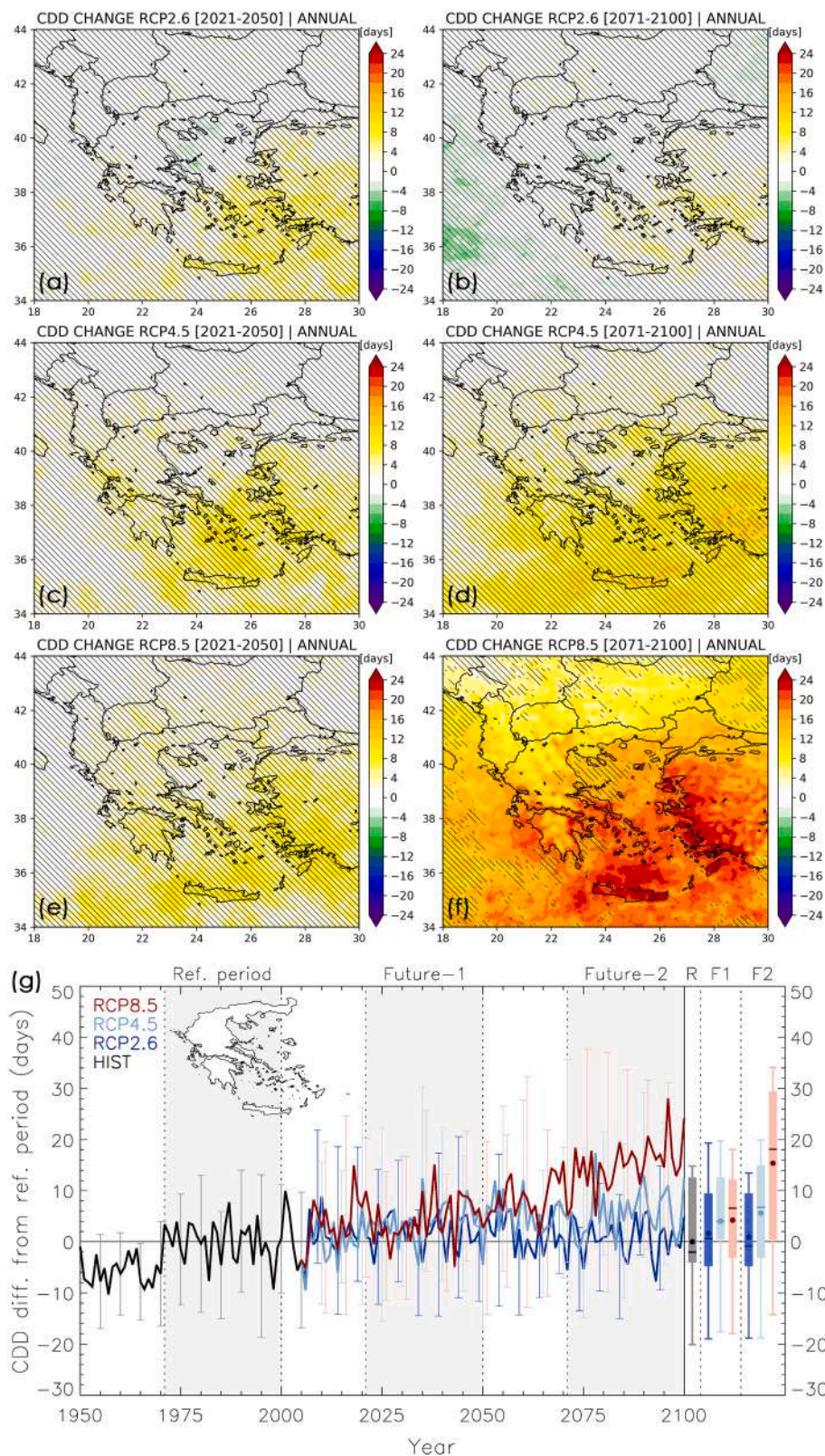


Fig. 7. The same as Fig. 2 but for CDD.

only (Fig. 7). Under RCP2.6 a small non-robust CDD increase/decrease of ± 4 days is indicated over different areas in southeastern Europe for both the future periods examined here. The largest CDD increase values (increased drought) appear over the southeastern part of the domain. The same stands for RCP4.5, with values up to 12 days in the near-future period and 16 days at the end-of-the-century period. For the near-future period, RCP8.5 changes are similar to the RCP4.5 ones for the same period and are in accordance to previous values given from Giannakopoulos et al. (2011) using a different reference period (1961–1990) and the SRES A1B scenario. At the end of the century, a strong increase of CDD from 8 up to 24 days is projected over the whole southeastern Europe. The largest increase appears over the central-southern Aegean Sea and continental areas around it. Specifically for Greece, Crete, and the Greek islands along the Turkish coastline (e.g., Mytilene and Rhodes) exhibit the highest CDD change values along with areas in the island of Euboea, in Attika and Peloponnese in line with Zanis et al. (2015) despite the fact that their analysis was based on the SRES A1B scenario and they used a different reference period (1961–1990). On average, over Greece, CDD is projected to increase marginally under RCP2.6 by less than 2–3% relative to the reference period in the near future and at the end of the century. Under RCP4.5, a small increase of 4 days (8%) is projected for the near-future period and 5.6 days (11%) for the end of the century. A small increase is also indicated under RCP8.5 for the near-future period (4.2 days or else 8%). On the contrary, at the end of the century, a significant CDD increase of 15.4 days (30%) is projected (Fig. 7g and Table 2). Similar changes in CDD for the near future and the end of the century were also reported by Zanis et al. (2015).

4. Conclusions

The essence of this work is the provision of an updated assessment of high resolution projected changes in climate-related parameters (TAS and PR) and indices (HD, TR, FD and CDD) over Greece and the surrounding areas (southeastern Europe) for the near future (2021–2050) and the end of the century (2071–2100) relative to a reference period (1971–2000). Our results are based on an ensemble of 11 high-resolution (0.11°) EURO-CORDEX RCM simulations covering the historical period 1950–2005 and the period 2006–2100 under three IPCC AR5 GHG concentration scenarios with strong mitigation (RCP2.6), medium mitigation (RCP4.5), and no mitigation (RCP8.5). Our main findings are summarized as follows:

- A statistically robust TAS increase is projected over the whole southeastern Europe domain both in the near future and at the end of the century under all the examined RCPs with the level of warming among the RCPs starting differentiating after 2030. The warming is larger over the continental part of Greece than over the sea.
- Over Greece, TAS is projected to increase by 1.2°C on average in the near future and 1.4°C at the end of the century under RCP2.6. For RCP4.5, TAS is projected to increase by 1.4°C and 2.3°C , respectively, while for RCP8.5, 1.6°C and 4.3°C . The TAS future change patterns are pretty similar throughout all the seasons with the annual change patterns, the projected changes being larger in summer particularly under RCP4.5 and RCP8.5.
- PR is projected to increase or decrease in the future over different areas within southeastern Europe, but the changes are generally non-robust. A robust decrease of PR is indicated over areas in Greece, southern Turkey and over the sea below $\sim 38^\circ\text{N}$ at the end of the century for RCP8.5 only.
- On average, PR is projected to decrease marginally over Greece by -3% (-0.1 mm day^{-1}) in the near future under all the examined RCPs. At the end of the century a decrease of -6% (-0.1 mm day^{-1}), and -16% (-0.4 mm day^{-1}) is projected under RCP4.5 and RCP8.5, respectively.
- The annual PR change patterns are mostly driven by the winter patterns with spring and autumn following. The projected decrease

of PR under RCP8.5 at the end of the century is of particular interest for the already dry summer season (-38% / -0.3 mm day^{-1}).

- Over Greece, HD is projected to increase on average from 5.5 days (108%) for RCP2.6 up to 7.4 days (145%) for RCP8.5 in the near future. At the end of the century, HD is not projected to change relative to the near-future period under RCP2.6. On the contrary, it is projected to increase by 11.8 days (more than double relative to the reference period) under RCP4.5 and 29.4 days (almost six times that of the reference period) under RCP8.5.
- TR is projected to increase on average by 14.7 days (69%) in the near future and remain at the same levels until the end of the century under RCP2.6. An increase of 16.9 days (79%) is projected for RCP4.5 and 19.7 days (92%) for RCP8.5 in the near future. At the end of the century the projected increase is 28.5 days (134%) under RCP4.5 and 57.9 days (almost three times that of the reference period) under RCP8.5, respectively.
- FD is projected to decrease on average by -9.7 days (-21%) in the near future and -12.4 days (-28%) at the end of the century under RCP2.6. For RCP4.5, the projected decrease is -11.6 days (-26%) for the near-future and -18.6 days (-41%) for the end-of-the-century period while for RCP8.5 it is -12.9 days (-29%) in the near future and -28.8 days (-64%) at the end of the century.
- CDD is projected to increase marginally by less than 2–3% in the near future and at the end of the century under RCP2.6. A small increase of 4 days (8%) is projected for the near-future period and 5.6 days (11%) for the end of the century under RCP4.5. A small increase of 4.2 days (8%) is also projected under RCP8.5 for the near-future period. On the contrary, at the end of the century, a significant CDD increase of 15.4 days (30%) is projected.
- Statistical robustness is largely indicated for the HD and FD future changes over the continental areas within southeastern Europe under all the examined RCPs. For TR robustness is indicated over the whole region while the change of CDD is statistically robust over the largest part of the region only for the end-of-the-century period under RCP8.5.

Overall, our results point towards a definitely warmer and possibly drier future, especially under RCP8.5. The produced ensemble of high resolution projected changes can serve as a basis for climate change impact studies for Greece. The availability of more EURO-CORDEX RCM simulations driven by the new generation CMIP6 GCMs and the new IPCC AR6 scenarios (Shared Socioeconomic Pathways; SSPs) would allow for an update our results in the future most probably suggesting an even warmer and drier future (Coppola et al., 2021).

Funding sources

This research received funding from the Action titled “National Network on Climate Change and its Impacts - CLIMPACT” which is implemented under the sub-project 3 of the project “Infrastructure of national research networks in the fields of Precision Medicine, Quantum Technology and Climate Change”, funded by the Public Investment Program of Greece, General Secretary of Research and Technology/Ministry of Development and Investments.

Declaration of Competing Interest

The authors declare that they have no known competing financial interests or personal relationships that could have appeared to influence the work reported in this paper.

Acknowledgements

The authors acknowledge funding from the Action titled “National Network on Climate Change and its Impacts - CLIMPACT” which is implemented under the sub-project 3 of the project “Infrastructure of

national research networks in the fields of Precision Medicine, Quantum Technology and Climate Change”, funded by the Public Investment Program of Greece, General Secretary of Research and Technology/Ministry of Development and Investments. Also, the authors acknowledge the World Climate Research Programme’s Working Group on Regional Climate, and the Working Group on Coupled Modelling, former coordinating body of CORDEX and responsible panel for CMIP5. Special thanks are expressed to the climate modelling groups for producing and making available their model output. The Earth System Grid Federation infrastructure an international effort led by the U.S. Department of Energy’s Program for Climate Model Diagnosis and Intercomparison, the European Network for Earth System Modelling and other partners in the Global Organisation for Earth System Science Portals (GO-ESSP) are also acknowledged. Finally, the authors acknowledge the E-OBS v23.1e dataset from the EU-FP6 project UERRA (<http://www.uerra.eu>) and the Copernicus Climate Change Service, and the data providers in the ECA&D project (<https://www.ecad.eu>). Results presented in this work have been produced using the Aristotle University of Thessaloniki (AUTH) high-performance computing infrastructure and resources.

Appendix A. Supplementary data

Supplementary data to this article can be found online at <https://doi.org/10.1016/j.atmosres.2022.106049>.

References

- Almazroui, M., Saeed, F., Saeed, S., Nazrul Islam, M., Ismail, M., Klutse, N.A.B., Siddiqui, M.H., 2020. Projected Change in Temperature and Precipitation over Africa from CMIP6. *Earth Syst. Environ.* 4, 455–475. <https://doi.org/10.1007/s41748-020-00161-x>.
- Almazroui, M., Islam, M.N., Saeed, F., Saeed, S., Ismail, M., Ehsan, M.A., Diallo, I., O’Brien, E., Ashfaq, M., Martínez-Castro, D., Cavazos, T., Cerezo-Mota, R., Tippet, M.K., Gutowski, W.J., Alfaro, E.J., Hidalgo, H.G., Vichot-Llano, A., Campbell, J.D., Kamil, S., Rashid, I.U., Sylla, M.B., Stephenson, T., Taylor, M., Barlow, M., 2021. Projected changes in Temperature and Precipitation over the United States, Central America, and the Caribbean in CMIP6 GCMs. *Earth Syst. Environ.* 5, 1–24. <https://doi.org/10.1007/s41748-021-00199-5>.
- Anagnostopoulou, C., 2017. Drought episodes over Greece as simulated by dynamical and statistical downscaling approaches. *Theor. Appl. Climatol.* 129, 587–605. <https://doi.org/10.1007/s00704-016-1799-5>.
- CCISC, 2011. *The environmental, economic and social impacts of climate change in Greece*. In: *Climate Change Impacts Study Committee*. Bank of Greece, Athens, pp. 1–520. ISBN:978-960-7032-49-2.
- Cook, B.I., Mankin, J.S., Marvel, K., Williams, A.P., Smerdon, J.E., Anchukaitis, K.J., 2020. Twenty-first Century Drought Projections in the CMIP6 Forcing scenarios. *Earth’s Future* 8. <https://doi.org/10.1029/2019EF001461>.
- Coppola, E., Nogherotto, R., Ciarlo, J.M., Giorgi, F., Meijgaard, E., Kadygrov, N., Iles, C., Corre, L., Sandstad, M., Somot, S., Nabat, P., Vautard, R., Levassasseur, G., Schwingshackl, C., Sillmann, J., Kjellström, E., Nikulin, G., Aalbers, E., Lenderink, G., Christensen, O.B., Boberg, F., Sørland, S.L., Demory, M., Bülow, K., Teichmann, C., Warrach-Sagi, K., Wulfmeyer, V., 2021. Assessment of the European climate Projections as simulated by the large EURO-CORDEX Regional and Global climate Model Ensemble. *Geophys. Res. Atmos.* 126 <https://doi.org/10.1029/2019JD032356>.
- Cornes, R.C., van der Schrier, G., van den Besselaar, E.J.M., Jones, P.D., 2018. An Ensemble Version of the E-OBS Temperature and Precipitation Data Sets. *J. Geophys. Res. Atmos.* 123, 9391–9409. <https://doi.org/10.1029/2017JD028200>.
- Cos, J., Doblas-Reyes, F., Jury, M., Marcos, R., Bretonnière, P.-A., Samsó, M., 2021. The Mediterranean climate change hotspot in the CMIP5 and CMIP6 projections. *Atmos. Chem. Phys. Dis.* <https://doi.org/10.5194/esd-2021-65>.
- Diffenbaugh, N.S., Pal, J.S., Giorgi, F., Gao, X., 2007. Heat stress intensification in the Mediterranean climate change hotspot. *Geophys. Res. Lett.* 34, L11706. <https://doi.org/10.1029/2007GL030000>.
- Eurostat, 2021. https://appsso.eurostat.ec.europa.eu/nui/show.do?dataset=n_ama_10_gdp&lang=en (Accessed 14 January 2022).
- Founda, D., Papadopoulos, K.H., Petrakis, M., Giannakopoulos, C., Good, P., 2004. Analysis of mean, maximum, and minimum temperature in Athens from 1897 to 2001 with emphasis on the last decade: trends, warm events, and cold events. *Glob. Planet. Chang.* 44, 27–38. <https://doi.org/10.1016/j.gloplacha.2004.06.003>.
- Founda, D., Varotsos, K.V., Pierros, F., Giannakopoulos, C., 2019. Observed and projected shifts in hot extremes’ season in the Eastern Mediterranean. *Glob. Planet. Chang.* 175, 190–200. <https://doi.org/10.1016/j.gloplacha.2019.02.012>.
- Gao, X., Pal, J.S., Giorgi, F., 2006. Projected changes in mean and extreme precipitation over the Mediterranean region from a high resolution double nested RCM simulation. *Geophys. Res. Lett.* 33, L03706. <https://doi.org/10.1029/2005GL024954>.
- Giannakopoulos, C., Le Sager, P., Bindi, M., Moriondo, M., Kostopoulou, E., Goodess, C.M., 2009. Climatic changes and associated impacts in the Mediterranean resulting from a 2 °C global warming. *Glob. Planet. Chang.* 68, 209–224. <https://doi.org/10.1016/j.gloplacha.2009.06.001>.
- Giannakopoulos, C., Kostopoulou, E., Varotsos, K.V., Tziotziou, K., Plitharas, A., 2011. An integrated assessment of climate change impacts for Greece in the near future. *Reg. Environ. Chang.* 11, 829–843. <https://doi.org/10.1007/s10113-011-0219-8>.
- Gibelin, A.-L., Déqué, M., 2003. Anthropogenic climate change over the Mediterranean region simulated by a global variable resolution model. *Clim. Dyn.* 20, 327–339. <https://doi.org/10.1007/s00382-002-0277-1>.
- Giorgi, F., 2006. Climate change hot-spots. *Geophys. Res. Lett.* 33, L08707. <https://doi.org/10.1029/2006GL025734>.
- Giorgi, F., Lionello, P., 2008. Climate change projections for the Mediterranean region. *Glob. Planet. Chang.* 63, 90–104. <https://doi.org/10.1016/j.gloplacha.2007.09.005>.
- Goubanov, K., Li, L., 2007. Extremes in temperature and precipitation around the Mediterranean basin in an ensemble of future climate scenario simulations. *Glob. Planet. Chang.* 57, 27–42. <https://doi.org/10.1016/j.gloplacha.2006.11.012>.
- Hadjinicolaou, P., Zittis, G., Lelieveld, J., 2017. Exploration of 12-km ERA-Interim Simulations from CORDEX over the Levant. In: Karacostas, T., Bais, A., Nastos, P.T. (Eds.), *Perspectives on Atmospheric Sciences*. Springer International Publishing, Cham, pp. 643–648.
- Hansen, J., Sato, M., Kharecha, P., Russell, G., Lea, D.W., Siddall, M., 2007. Climate change and trace gases. *Phil. Trans. R. Soc. A* 365, 1925–1954. <https://doi.org/10.1098/rsta.2007.2052>.
- Haylock, M.R., Hofstra, N., Klein Tank, A.M.G., Klok, E.J., Jones, P.D., New, M., 2008. A European daily high-resolution gridded data set of surface temperature and precipitation for 1950–2006. *J. Geophys. Res.* 113, D20119. <https://doi.org/10.1029/2008JD010201>.
- IPCC, 2013. In: Stocker, T.F., Qin, D., Plattner, G.-K., Tignor, M., Allen, S.K., Boschung, J., Midgley, P.M. (Eds.), *Climate Change 2013: The Physical Science Basis*. Contribution of Working Group I to the Fifth Assessment Report of the Intergovernmental Panel on Climate Change. Cambridge University Press, Cambridge, United Kingdom and New York, NY, USA, p. 1535.
- IPCC, 2021. In: Masson-Delmotte, V., Zhai, P., Pirani, A., Connors, S.L., Péan, C., Berger, S., Zhou, B. (Eds.), *Climate Change 2021: The Physical Science Basis*. Contribution of Working Group I to the Sixth Assessment Report of the Intergovernmental Panel on Climate Change. Cambridge University Press, in press.
- Jacob, D., Petersen, J., Eggert, B., Alias, A., Christensen, O.B., Bouwer, L.M., Braun, A., Colette, A., Déqué, M., Georgievski, G., Georgopoulou, E., Gobiet, A., Menut, L., Nikulin, G., Haensler, A., Hempelmann, N., Jones, C., Keuler, K., Kovats, S., Kröner, N., Kotlarski, S., Kriegsmann, A., Martin, E., van Meijgaard, E., Moseley, C., Pfeifer, S., Preuschmann, S., Radermacher, C., Radtke, K., Reich, D., Rounsevell, M., Samuelsson, P., Somot, S., Soussana, J.-F., Teichmann, C., Valentini, R., Vautard, R., Weber, B., Yiou, P., 2014. EURO-CORDEX: new high-resolution climate change projections for European impact research. *Reg. Environ. Chang.* 14, 563–578. <https://doi.org/10.1007/s10113-013-0499-2>.
- Jacob, D., Teichmann, C., Sobolowski, S., Katragkou, E., Anders, I., Belda, M., Benestad, R., Boberg, F., Buonomo, E., Cardoso, R.M., Casanueva, A., Christensen, O.B., Christensen, J.H., Coppola, E., De Cruz, L., Davin, E.L., Dobler, A., Domínguez, M., Fealy, R., Fernandez, J., Gaertner, M.A., García-Díez, M., Giorgi, F., Gobiet, A., Goergen, K., Gómez-Navarro, J.J., Alemán, J.J.G., Gutiérrez, C., Gutiérrez, J.M., Güttler, I., Haensler, A., Halenka, T., Jerez, S., Jiménez-Guerrero, P., Jones, R.G., Keuler, K., Kjellström, E., Knist, S., Kotlarski, S., Maraun, D., van Meijgaard, E., Mercogliano, P., Montávez, J.P., Navarra, A., Nikulin, G., de Noblet-Ducoudré, N., Panitz, H.-J., Pfeifer, S., Piazza, M., Pichelli, E., Pietikäinen, J.-P., Prein, A.F., Preuschmann, S., Reich, D., Rockel, B., Romera, R., Sánchez, E., Sieck, K., Soares, P.M.M., Somot, S., Srncel, L., Sorland, S.L., Termonia, P., Truhetz, H., Vautard, R., Warrach-Sagi, K., Wulfmeyer, V., 2020. Regional climate downscaling over Europe: perspectives from the EURO-CORDEX community. *Reg. Environ. Chang.* 20, 51. <https://doi.org/10.1007/s10113-020-01606-9>.
- Katragkou, E., García-Díez, M., Vautard, R., Sobolowski, S., Zanis, P., Alexandri, G., Cardoso, R.M., Colette, A., Fernandez, J., Gobiet, A., Goergen, K., Karacostas, T., Knist, S., Mayer, S., Soares, P.M.M., Pytharoulis, I., Tegoulis, I., Tserkedakis, A., Jacob, D., 2015. Regional climate hindcast simulations within EURO-CORDEX: evaluation of a WRF multi-physics ensemble. *Geosci. Model Dev.* 8, 603–618. <https://doi.org/10.5194/gmd-8-603-2015>.
- Kotlarski, S., Keuler, K., Christensen, O.B., Colette, A., Déqué, M., Gobiet, A., Goergen, K., Jacob, D., Lüthi, D., van Meijgaard, E., Nikulin, G., Schär, C., Teichmann, C., Vautard, R., Warrach-Sagi, K., Wulfmeyer, V., 2014. Regional climate modeling on European scales: a joint standard evaluation of the EURO-CORDEX RCM ensemble. *Geosci. Model Dev.* 7, 1297–1333. <https://doi.org/10.5194/gmd-7-1297-2014>.
- Lelieveld, J., Hadjinicolaou, P., Kostopoulou, E., Chenoweth, J., El Maayar, M., Giannakopoulos, C., Hannides, C., Lange, M.A., Tanarhte, M., Tyrlis, E., Xoplaki, E., 2012. Climate change and impacts in the Eastern Mediterranean and the Middle East. *Clim. Chang.* 114, 667–687. <https://doi.org/10.1007/s10584-012-0418-4>.
- Lelieveld, J., Hadjinicolaou, P., Kostopoulou, E., Giannakopoulos, C., Pozzer, A., Tanarhte, M., Tyrlis, E., 2014. Model projected heat extremes and air pollution in the eastern Mediterranean and Middle East in the twenty-first century. *Reg. Environ. Chang.* 14, 1937–1949. <https://doi.org/10.1007/s10113-013-0444-4>.
- Mann, H.B., Whitney, D.R., 1947. On a Test of whether one of two Random Variables is Stochastically Larger than the other. *Ann. Math. Stat.* 18, 50–60. <https://doi.org/10.1214/aoms/1177730491>.
- MedECC, 2020. In: Cramer, W., Guiot, J., Marini, K. (Eds.), *Climate and Environmental Change in the Mediterranean Basin - Current Situation and Risks for the Future*. First Mediterranean Assessment Report. Union for the Mediterranean, Plan Bleu, UNEP/

- MAP, Marseille, France, p. 632. ISBN:978-2-9577416-0-1. https://zenodo.org/record/4768833#.YUi3zH2_yUk.
- Moss, R.H., Edmonds, J.A., Hibbard, K.A., Manning, M.R., Rose, S.K., van Vuuren, D.P., Carter, T.R., Emori, S., Kainuma, M., Kram, T., Meehl, G.A., Mitchell, J.F.B., Nakicenovic, N., Riahi, K., Smith, S.J., Stouffer, R.J., Thomson, A.M., Weyant, J.P., Wilbanks, T.J., 2010. The next generation of scenarios for climate change research and assessment. *Nature* 463, 747–756. <https://doi.org/10.1038/nature08823>.
- Nastos, P.T., Kapsomenakis, J., 2015. Regional climate model simulations of extreme air temperature in Greece. Abnormal or common records in the future climate? *Atmos. Res.* 152, 43–60. <https://doi.org/10.1016/j.atmosres.2014.02.005>.
- Nastos, P.T., Zerefos, C.S., 2009. Spatial and temporal variability of consecutive dry and wet days in Greece. *Atmos. Res.* 94, 616–628. <https://doi.org/10.1016/j.atmosres.2009.03.009>.
- Nastos, P.T., Philandras, C.M., Kapsomenakis, J., Eleftheratos, K., 2011. Variability and trends of mean maximum and mean minimum air temperature in Greece from ground-based observations and NCEP–NCAR reanalysis gridded data. *Int. J. Remote Sens.* 32, 6177–6192. <https://doi.org/10.1080/01431161.2010.507798>.
- Pfeifer, S., Bülow, K., Gobiet, A., Häsler, A., Mudelsee, M., Otto, J., Rechid, D., Teichmann, C., Jacob, D., 2015. Robustness of Ensemble climate Projections Analyzed with climate Signal Maps: Seasonal and Extreme Precipitation for Germany. *Atmosphere* 6, 677–698. <https://doi.org/10.3390/atmos6050677>.
- Politi, N., Vlachogiannis, D., Sfetos, A., Nastos, P.T., 2021. High-resolution dynamical downscaling of ERA-Interim temperature and precipitation using WRF model for Greece. *Clim. Dyn.* 57, 799–825. <https://doi.org/10.1007/s00382-021-05741-9>.
- Riahi, K., Rao, S., Krey, V., Cho, C., Chirkov, V., Fischer, G., Kindermann, G., Nakicenovic, N., Rafaj, P., 2011. RCP 8.5—a scenario of comparatively high greenhouse gas emissions. *Clim. Chang.* 109, 33–57. <https://doi.org/10.1007/s10584-011-0149-y>.
- Spinoni, J., Barbosa, P., Bucchignani, E., Cassano, J., Cavazos, T., Christensen, J.H., Christensen, O.B., Coppola, E., Evans, J., Geyer, B., Giorgi, F., Hadjinicolaou, P., Jacob, D., Kattafy, J., Koenigk, T., Laprise, R., Lennard, C.J., Kurnaz, M.L., Li, D., Llopart, M., McCormick, N., Naumann, G., Nikulin, G., Ozturk, T., Panitz, H.-J., Porfiro da Rocha, R., Rockel, B., Solman, S.A., Syktus, J., Tangang, F., Teichmann, C., Vautard, R., Vogt, J.V., Winger, K., Zittis, G., Dosio, A., 2020. Future Global Meteorological Drought Hot spots: a Study based on CORDEX Data. *J. Clim.* 33, 3635–3661. <https://doi.org/10.1175/JCLI-D-19-0084.1>.
- Taylor, K.E., Stouffer, R.J., Meehl, G.A., 2012. An Overview of CMIP5 and the Experiment Design. *Bull. Am. Meteorol. Soc.* 93, 485–498. <https://doi.org/10.1175/BAMS-D-11-00094.1>.
- Thomson, A.M., Calvin, K.V., Smith, S.J., Kyle, G.P., Volke, A., Patel, P., Delgado-Arias, S., Bond-Lamberty, B., Wise, M.A., Clarke, L.E., Edmonds, J.A., 2011. RCP4.5: a pathway for stabilization of radiative forcing by 2100. *Clim. Chang.* 109, 77–94. <https://doi.org/10.1007/s10584-011-0151-4>.
- Tolika, K., Zanis, P., Anagnostopoulou, C., 2012. Regional climate change scenarios for Greece: future temperature and precipitation projections from ensembles of RCMs. *Global NEST J.* 14, 407–421. <https://doi.org/10.30955/gnj.000776>.
- van Vuuren, D.P., Edmonds, J., Kainuma, M., Riahi, K., Thomson, A., Hibbard, K., Hurtt, G.C., Kram, T., Krey, V., Lamarque, J.-F., Masui, T., Meinshausen, M., Nakicenovic, N., Smith, S.J., Rose, S.K., 2011a. The representative concentration pathways: an overview. *Clim. Chang.* 109, 5–31. <https://doi.org/10.1007/s10584-011-0148-z>.
- van Vuuren, D.P., Stehfest, E., den Elzen, M.G.J., Kram, T., van Vliet, J., Deetman, S., Isaac, M., Klein Goldewijk, K., Hof, A., Mendoza Beltran, A., Oostenrijk, R., van Ruijven, B., 2011b. RCP2.6: exploring the possibility to keep global mean temperature increase below 2°C. *Clim. Chang.* 109, 95–116. <https://doi.org/10.1007/s10584-011-0152-3>.
- Vautard, R., Gobiet, A., Jacob, D., Belda, M., Colette, A., Déqué, M., Fernández, J., García-Díez, M., Goergen, K., Güttler, I., Halenka, T., Karacostas, T., Katragkou, E., Keuler, K., Kotlarski, S., Mayer, S., van Meijgaard, E., Nikulin, G., Patarčić, M., Scinocca, J., Sobolowski, S., Suklitsch, M., Teichmann, C., Warrach-Sagi, K., Wulfmeyer, V., Yiou, P., 2013. The simulation of European heat waves from an ensemble of regional climate models within the EURO-CORDEX project. *Clim. Dyn.* 41, 2555–2575. <https://doi.org/10.1007/s00382-013-1714-z>.
- Xue, Y., Janjic, Z., Dudhia, J., Vasic, R., De Sales, F., 2014. A review on regional dynamical downscaling in intraseasonal to seasonal simulation/prediction and major factors that affect downscaling ability. *Atmos. Res.* 147–148, 68–85. <https://doi.org/10.1016/j.atmosres.2014.05.001>.
- Zanis, P., Kapsomenakis, I., Philandras, C., Douvis, K., Nikolakis, D., Kanellopoulou, E., Zerefos, C., Repapis, C., 2009. Analysis of an ensemble of present day and future regional climate simulations for Greece. *Int. J. Climatol.* 29, 1614–1633. <https://doi.org/10.1002/joc.1809>.
- Zanis, P., Katragkou, E., Ntogras, C., Marougianni, G., Tsikerdekis, A., Feidas, H., Anadranistakis, E., Melas, D., 2015. Transient high-resolution regional climate simulation for Greece over the period 1960–2100: evaluation and future projections. *Clim. Res.* 64, 123–140. <https://doi.org/10.3354/cr01304>.
- Zerefos, C., Repapis, C., Giannakopoulos, C., Kapsomenakis, J., Papanikolaou, D., 2011. The climate of the eastern Mediterranean and Greece: Past, present and future. In: *The Environmental, Economic and Social Impacts of Climate Change in Greece. Climate Change Impacts Study Committee. Bank of Greece, Athens*, pp. 1–126.
- Zittis, G., Hadjinicolaou, P., Klangidou, M., Proestos, Y., Lelieveld, J., 2019. A multi-model, multi-scenario, and multi-domain analysis of regional climate projections for the Mediterranean. *Reg. Environ. Chang.* 19, 2621–2635. <https://doi.org/10.1007/s10113-019-01565-w>.
- Zittis, G., Bruggeman, A., Lelieveld, J., 2021. Revisiting future extreme precipitation trends in the Mediterranean. *Weather Climate Extremes* 34, 100380. <https://doi.org/10.1016/j.wace.2021.100380>.